Available online at www.sciencedirect.com
SciVerse ScienceDirect
Ceramics International 38 (2012) 1915–1920
CERAMICS INTERNATIONAL
www.elsevier.com/locate/ceramint

Doping behaviors of NiO and Nb_2O_5 in $BaTiO_3$ and dielectric properties of $BaTiO_3$-based X7R ceramics

Lingxia Li [*], Ruixue Fu, Qingwei Liao, Lujie Ji

School of Electronic and Information Engineering, Tianjin University, Tianjin 300072, China

Received 28 June 2011; received in revised form 9 October 2011; accepted 10 October 2011
Available online 15 October 2011

Abstract

Doping behaviors of NiO and Nb_2O_5 in $BaTiO_3$ in two doping ways and dielectric properties of $BaTiO_3$-based X7R ceramics were investigated. When doped in composite form, the additions rendered higher solubility than that doped separately due to the identical valence between the complex $(Ni_{1/3}^{2+}Nb_{2/3}^{5+})^{4+}$ and Ti^{4+}. NiO–Nb_2O_5 composite oxide was more effective in broadening dielectric constant peaks which was responsible for the temperature-stability of $BaTiO_3$ ceramics. A reduction in grain size was observed in the specimens with 0.5–0.8 mol% NiO–Nb_2O_5 composite oxide, whereas the abnormal growth of individual grains took place in the 1.0 mol% NiO–Nb_2O_5 composite oxide-doped specimen. When the specimen of $BaTiO_3$ doped with 0.8 mol% NiO–Nb_2O_5 composite oxide was sintered at 1300 °C for 1.5 h in air, good dielectric properties were obtained and the requirement of (EIA) X7R specification with a dielectric constant of 4706 and dielectric loss lower than 1.5% were satisfied.

Keywords: $BaTiO_3$; NiO–Nb_2O_5 composite oxide; Solubility; Broadening peaks; X7R

1. Introduction

X7R multi-layer ceramic capacitors (MLCCs) have been widely used for miniaturization of electronic components. $BaTiO_3$-based X7R dielectric materials mainly used to prepare MLCCs had attracted much attention due to their high permittivity and excellent dielectric constant thermal stability (-55 °C to 125 °C, $\Delta C/C \leq 15\%$).

Many investigations have been performed in order to obtain a superior material with high dielectric constant and X7R characteristics. The commonly used methods for improving the dielectric properties of $BaTiO_3$ include incorporation of additives (Nb_2O_5, MgO, Co_2O_3 and Yb_2O_3) [1–4], specialized synthesis of $BaTiO_3$ [5,6] and grain size distribution [7–9] and sintering process [10,11]. It has been known that achieving a good dielectric property through addition of dopants was most commonly used by researchers, such as $BaTiO_3$–Nb_2O_5–ZnO [12], $BaTiO_3$–Nb_2O_5–Co_3O_4 [13], and $BaTiO_3$–Nb_2O_5–Ni_2O_3 [14] systems. As many researchers have reported [15–18], NiO and Nb_2O_5 additions can broaden dielectric constant peaks and improve dielectric properties of $BaTiO_3$-based ceramics. However, doping Nb_2O_5, NiO in the form of composite oxide showed great effects in improving dielectric properties of the $BaTiO_3$ ceramics compared to doping Nb_2O_5, NiO separately, which has not been reported.

In this paper, the solubility of NiO, Nb_2O_5 in $BaTiO_3$ and the effects on dielectric peak-broadening of $BaTiO_3$ by two doping methods (doping NiO–Nb_2O_5 as composite oxide and doping NiO, Nb_2O_5 separately) was investigated. The doping mechanism of NiO, Nb_2O_5 and the dielectric peak-broadening mechanism of NiO–Nb_2O_5 composite oxide in $BaTiO_3$-based system were elucidated precisely. Moreover, through the first doping methods, the $BaTiO_3$-based X7R ceramic with satisfactory dielectric properties was synthesized using conventional mixed-oxide method, which can help develop novel temperature-stable dielectric materials for X7R MLCCs.

2. Experimental procedure

$BaTiO_3$ (particle size about 0.4 μm) powders were synthesized by co-precipitation method and calcined at 1080 °C for 2 h. Nb_2O_5 (99.99%, Jiujiang Tanbre's Smeltery,

---

[*] Corresponding author. Tel.: +86 22 27402838; fax: +86 22 27401233.
E-mail address: lilingxia@tju.edu.cn (L. Li).

0272-8842/$36.00 © 2011 Elsevier Ltd and Techna Group S.r.l. All rights reserved.
doi:10.1016/j.ceramint.2011.10.020

China), NiO (99.0%, Tianjin Chemical Reagent Company, China) were used as the starting materials. NiO and Nb_2O_5 powders were mixed and milled in deionized water and zirconia milling media for 4 h, then dried and calcined at 1000 °C for 2 h to form NiO–Nb_2O_5 composite oxide. The NiO–Nb_2O_5 composite oxide powders and $BaTiO_3$ were milled again and dried to form composite (hereafter referred to as composition A). The uncalcined NiO and Nb_2O_5 were milled with $BaTiO_3$ directly and dried to form composite (hereafter referred to as composition B). The milled powders were granulated by mixing them with a 7 wt.% binder, and then the granules were pressed into disks with 20 mm in diameter and $1 > 1.5$ mm in thickness. These samples were conventionally sintered at 1300 °C in air for 1.5 h.

After samples were fired at 850 °C with Ag electrodes on both surfaces, the capacitances of samples were measured from −55 °C to 150 °C with LCR (HP4278A) at 1 kHz and 1 V rms. The temperature was controlled by GZ-ESPEC oven. The dielectric constant (ε_r) and the variation of capacity ($\Delta C/C_{20\,^{\circ}\mathrm{C}}$ (%)) were calculated from the measured capacitances. Insulation resistance was measured using a high resistance meter (Super-High Resistance Meter Model ZC36) at room temperature. D/MAX-B Model X-ray diffractometer with Cu Kα radiation at 40 kV and 40 mA settings was used to analyze the phase composition of ceramics. The dielectric loss was measured at 1 kHz with LCR (HP4278A). Microstructural properties such as grain size distribution and morphology were examined using a Phillips XL30 scanning electron microscope (SEM).

3. Results and discussion

3.1. Solubility analysis

Fig. 1(a) and (b) shows the XRD patterns of composition A (doping NiO, Nb_2O_5 as composite oxide) and composition B (doping NiO, Nb_2O_5 separately) samples sintering at 1300 °C for 1.5 h, respectively. The compositions of A1–A4 and B1–B4 were shown in Table 1.

The X-ray diffraction patterns of composition A and composition B both showed a pseudo-cubic structure with a single peak of (2 0 0). The secondary phase ($Ba_6Ti_{17}O_{40}$ (JCPDF 77-1566)) was detected when 1.0 mol% NiO–Nb_2O_5 composite oxide was added to $BaTiO_3$, while it was already observed when NiO, Nb_2O_5 were added separately at 0.8 mol%. Therefore, it was indicated that the solubility limit of NiO, Nb_2O_5 in $BaTiO_3$ were different between the two different doping methods. NiO, Nb_2O_5 had relatively larger solubility limit by doping NiO, Nb_2O_5 as composite oxide.

When NiO, Nb_2O_5 were compounded into $BaTiO_3$-based ceramics system, Ni^{2+} and Nb^{5+} were apt to replace Ti^{4+} due to their similar ionic radius [17–20]. The effects of Nb and Ni elements were different. Since the charge of Ni^{2+} ion was lower than that of Ti^{4+} ion, the Ni^{2+} ion acted as an acceptor to $BaTiO_3$, whereas Nb element was a donor for its relatively higher valence. The defect reactions were shown as follows:

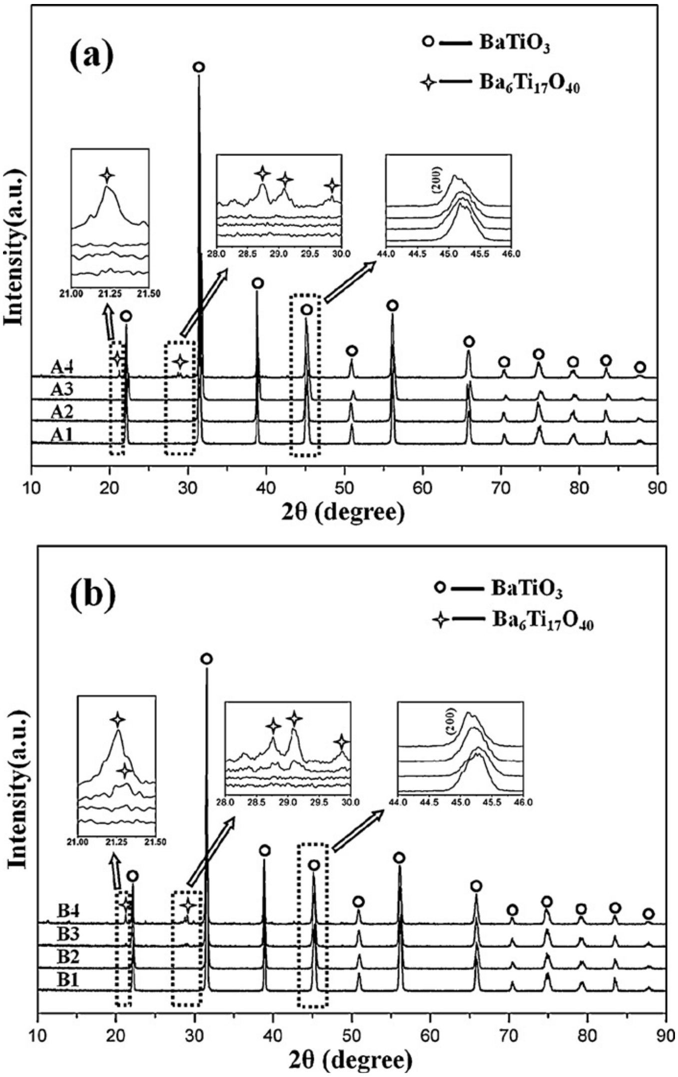

Fig. 1. XRD patterns of samples (a) composition A (A1–A4) and (b) composition B (B1–B4) sintered at 1300 °C.

$$NiO = Ni''_{Ti} + V_o^{\bullet\bullet} + Oo \tag{1}$$

$$2Nb_2O_5 = 4Nb_{Ti}^{\bullet} + V_{Ti}'''' + 10Oo \tag{2}$$

Table 1
Sample compositions (mol%).

Composition	$BaTiO_3$	Nb_2O_5	NiO
A1	100	0.5 NiO–0.5 Nb_2O_5 composite oxide	
A2	100	0.7 NiO–0.7 Nb_2O_5 composite oxide	
A3	100	0.8 NiO–0.8 Nb_2O_5 composite oxide	
A4	100	1.0 NiO–1.0 Nb_2O_5 composite oxide	
B1	100	0.5	0.5
B2	100	0.7	0.7
B3	100	0.8	0.8
B4	100	1.0	1.0

In composition B, the low solubility of NiO, Nb_2O_5 in $BaTiO_3$ was related to different valence states among Ni^{2+}, Nb^{5+} and Ti^{4+}. The differences of valence among Ni^{2+}, Nb^{5+} and Ti^{4+} ions resulted in the appearance of the vacancies, as Eqs. (1) and (2) shown. The generation of vacancies resulted in the distortion of the lattice. With larger lattice distortion, the energy of lattice distortion would be higher, which led to instability of the crystal structure. And the instability limited the further diffusion of the doping ions [21], which resulted in the relatively low solubility of NiO, Nb_2O_5 in $BaTiO_3$ of composition B.

In composition A, when NiO and Nb_2O_5 were doped as NiO–Nb_2O_5 composite oxide, the Ni^{2+} and Nb^{5+} ions would replace the Ti^{4+} by forming the composite cation of $(Ni_{1/3}{}^{2+}Nb_{2/3}{}^{5+})^{4+}$. The ionic radius of $(Ni_{1/3}{}^{2+}Nb_{2/3}{}^{5+})^{4+}$ was close to the radius of Ti^{4+} (The effective radius of Ti^{4+} was 0.061 nm and $(Ni_{1/3}{}^{2+}Nb_{2/3}{}^{5+})^{4+}$ was 0.066 nm in the 6-fold coordination [22]). Furthermore, the valence of the complex $(Ni_{1/3}{}^{2+}Nb_{2/3}{}^{5+})^{4+}$ was identical to Ti^{4+}. When NiO and Nb_2O_5 were doped in $BaTiO_3$ as composite, the ions Ni^{2+} and Nb^{5+} substituted Ti site as follows:

$$3BaO + NiO + Nb_2O_5 = 3Ba_{Ba} + Ni''_{Ti} + 2Nb^{\bullet}_{Ti} + 9O_O \qquad (3)$$

This reaction may exclude the energetically unfavorable defect species such as V_{Ti}'''' in Eq. (2). Thus, the composite source of NiO and Nb_2O_5 creates favorable defect species as shown in Eq. (3), leading to higher solubility in composition A.

3.2. Dielectric peak-broadening effects

Fig. 2(a) and (b) presents the temperature dependence of the dielectric constant ε_r of the composition A (A1–A4) and composition B (B1–B4) ceramics measuring at 1 kHz.

Two dielectric constant peaks were observed in the dielectric constant–temperature curves (ε_r–T curves) in Fig. 2(a) and (b). This phenomenon was associated with the chemically inhomogeneous structure (the "core–shell" structure) of doped $BaTiO_3$. The Curie dielectric peak (at about 130 °C) was determined by the ferroelectric–paraelectric transition of grain core, whereas the secondary peak at lower temperature was due to strong chemical inhomogeneity of grain shell [23]. It was apparent that the flattening ability of additives in this system was associated with the inhomogeneous chemical distribution of grain shell in the matrix grains.

It was apparent that the secondary dielectric constant peak was more obvious and broader in Fig. 2(a) than in Fig. 2(b). The results indicate that the NiO–Nb_2O_5 composite oxide was very effective to flatten the dielectric constant–temperature curve at low temperature. Since the $(Ni_{1/3}{}^{2+}Nb_{2/3}{}^{5+})^{4+}$ cation easily diffused into the crystal lattice in composition A to form the chemically inhomogeneous structure of grain shell. A relatively large volume fraction of the grain shell resulted in the obvious dielectric constant peak at low temperature.

As show in Fig. 2(a), the ε_r–T curves became broader with the increasing amount of $(Ni_{1/3}{}^{2+}Nb_{2/3}{}^{5+})^{4+}$ addition (from 0.5 mol% to 1.0 mol%). A certain amount of $(Ni_{1/3}{}^{2+}Nb_{2/3}{}^{5+})^{4+}$ ions substituting for Ti^{4+} ions formed the chemically inhomogeneous structure and the compositional inhomogeneity might induce diffuse phase transition characteristics, which resulted in a multi-peaks character over a relatively wide temperature range. The combination and overlapping of multi-peaks contributed to the broad peaks of ε_r–T curves. And the diffuse phase transition behavior of this system became more pronounced with increasing amount of $(Ni_{1/3}{}^{2+}Nb_{2/3}{}^{5+})^{4+}$. So the overall dielectric peaks of compositions A was broadened in the whole measurement temperature when the amount of $(Ni_{1/3}{}^{2+}Nb_{2/3}{}^{5+})^{4+}$ increased.

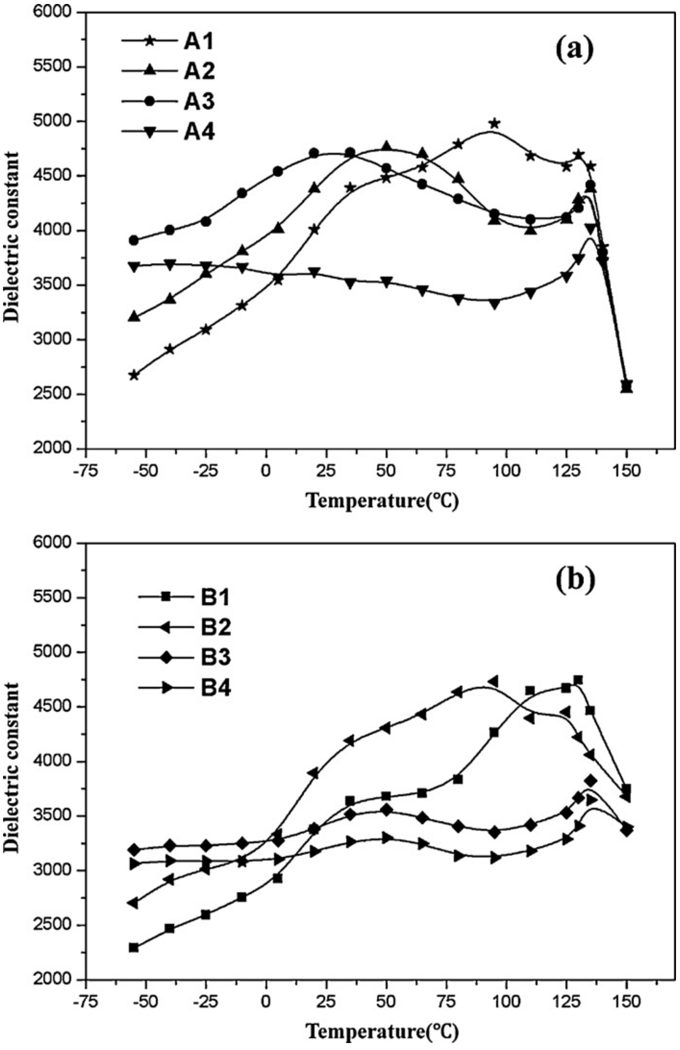

Fig. 2. Temperature dependence of dielectric constant of samples (a) composition A (A1–A4) and (b) composition B (B1–B4) sintered at 1300 °C for 1.5 h.

3.3. Microstructure and dielectric properties of composition A

According to the previous discussion, composition A showed a preferable dielectric peaks broadening effect, which was helpful to improve the dielectric properties of $BaTiO_3$-based ceramics. Therefore, the microstructure and dielectric properties of composition A samples would be further analyzed.

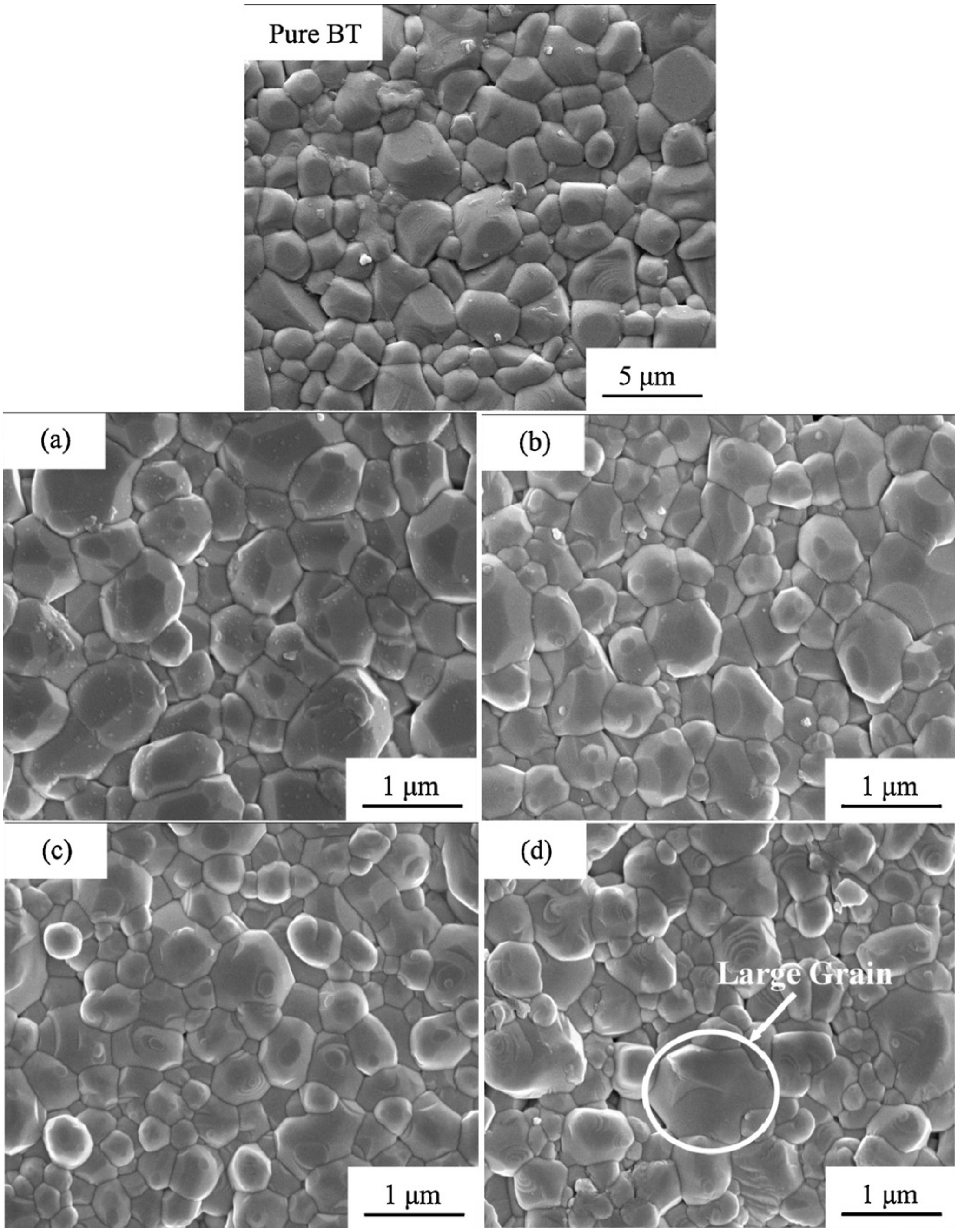

Fig. 3. SEM micrographs of pure $BaTiO_3$ and composition A (A1–A4): (a) A1, (b) A2, (c) A3, (d) A4 samples sintered at 1300 °C.

Fig. 3 showed the microstructures of pure $BaTiO_3$ and composition A specimens after sintering at 1300 °C for 1.5 h in air. The average grain sizes of sintered ceramics were obtained from the SEM micrographs by the linear interception method [24], as shown in Table 2. The average size of $BaTiO_3$ grains in the pure $BaTiO_3$ specimens grew to 2.62 μm. With increasing additions content, the grains of the samples became more perfect and the grain sizes decreased, when the content of NiO–Nb_2O_5 composite oxide was less than 0.8 mol%, indicating that the addition of the $(Ni_{1/3}{}^{2+}Nb_{2/3}{}^{5+})^{4+}$ ions inhibited the grain growth of $BaTiO_3$ in these samples. However, when the NiO–Nb_2O_5 composite oxide content increased further to 1.0 mol%, a slight increase in average grain size was observed in Table 2.

Table 2
Average grain sizes of pure $BaTiO_3$ and composition A (A1–A4) samples sintered at 1300 °C for 1.5 h.

Samples	Average grain size (μm)
Pure BT	2.62
A1	0.76
A2	0.61
A3	0.53
A4	0.56

Table 3
Dielectric properties of composition A (A1–A4) samples.

Samples	Dielectric constant (ε_r)	Dielectric loss (tgδ%)	Insulation resistance (ρ_v, 10^{12} Ω cm)	Temperature coefficient of capacitance ($\Delta C/C_{20\,^\circ C}$ (%))	
				−55 °C	125 °C
A1	4010	1.732	2.1	−33.2	14.2
A2	4380	1.356	2.8	−26.8	−6.4
A3	4706	1.230	3.7	−14.6	−12.5
A4	3627	0.838	5.0	1.3	−1.1

This was related to the formation of individual large grains as shown in Fig. 3(d). As NiO–Nb_2O_5 composite oxide content increased to 1.0 mol%, secondary phase began to occur which was proved by XRD analysis. However, it was hard to observe the secondary phase grains by SEM due to the formation of small amount of secondary phase. The formation of liquid phase of $Ba_6Ti_{17}O_{40}$, might be responsible for the formation of large grains.

The main dielectric properties of composition A specimens were summarized in Table 3. The dielectric constant (ε_r) at room temperature initially increased with increasing NiO–Nb_2O_5 composite oxide content up to 0.8 mol% and then decreased. Consequently, the sample with 0.8 mol% composite oxide had ε_r as high as 4706, which was higher than that of the $BaTiO_3$–Ni_2O_3–Nb_2O_5 system [14]. The high dielectric constant was related to the second broad peak near room temperature and homogeneous fine-grained microstructures as shown in Fig. 3(c). When NiO–Nb_2O_5 composite oxide content increased to 1.0 mol%, room temperature constant decreased pronouncedly. This was related to the increase of non-ferroelectric phase of grain shell and the abnormal growth of individual grain for the emergence of the secondary phase, when the amount of NiO–Nb_2O_5 composite oxide added was beyond the solubility.

The room temperature dielectric loss (tgδ) monotonically decreased with increasing content of NiO–Nb_2O_5 composite oxide. This was owing to the polarization actually decreased due to the substitution between Ti^{4+} and $(Ni_{1/3}Nb_{2/3})^{4+}$ and small ionic polarization leaded to the decrease in dielectric loss. For the samples doped with 0.7, 0.8, 1.0 mol% NiO–Nb_2O_5 composite oxide, dielectric loss values were less than 1.5% and the insulation resistances were higher than 10^{12} Ω cm.

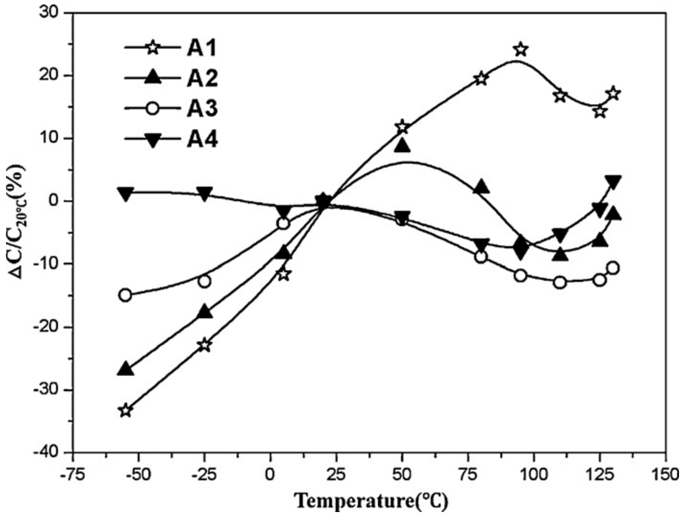

Fig. 4. $\Delta C/C_{20\,^\circ C}$–$T$ curves of composition A (A1–A4) samples.

$\Delta C/C_{20\,^\circ C}$–$T$ curves of composition A ceramics were presented in Fig. 4. The $\Delta C/C_{20\,^\circ C}$–$T$ curves were flattened and peaks were broadened noticeably with the amount of additions increasing. Especially the variation rate of capacity of samples with 0.8 mol% NiO–Nb_2O_5 composition doping was already lower than ±15%, which satisfied the X7R specification with a high dielectric constant. The sample exhibited satisfied variation of capacity when the amount of dopants increased up to 1.0 mol%, but the room temperature dielectric constant was relatively low about 3600.

It can conclude that the ceramics with 0.8 mol% NiO–Nb_2O_5 composition oxide content had the maximum room temperature permittivity (4706) and the low dielectric loss (0.0123). The ceramic had better dielectric temperature stability with the temperature ranging from −55 °C to 125 °C, and satisfied the specification of (EIA) X7R capacitor. The NiO–Nb_2O_5 composite oxide was very helpful in improving the overall dielectric properties of $BaTiO_3$-based ceramics.

4. Conclusions

Doping behaviors of NiO and Nb_2O_5 in $BaTiO_3$ and dielectric properties of $BaTiO_3$-based X7R ceramics have been investigated. When NiO and Nb_2O_5 doped as composite oxide, the Ni^{2+}, Nb^{5+} cations would replace the Ti site by forming the composite cation of $(Ni_{1/3}{}^{2+}Nb_{2/3}{}^{5+})^{4+}$. From the solubility analysis results, Ni^{2+}, Nb^{5+} cations were easier to diffuse into the crystal lattice by using the NiO–Nb_2O_5 composite oxide as dopants, which was attributed to the identity of $(Ni_{1/3}{}^{2+}Nb_{2/3}{}^{5+})^{4+}$ and Ti^{4+}. NiO and Nb_2O_5 doping as composite oxide were more effective in broadening dielectric peaks and improving dielectric properties of the $BaTiO_3$-based ceramics. With increasing NiO–Nb_2O_5 composition oxide content (from 0.5 mol% to 0.8 mol%), the grain size of $BaTiO_3$ decreased, whereas the abnormal growth of individual grains took place in the 1.0 mol% composition oxide-doped specimen. The abnormal growth in grain size was related to presence of the second phase, $Ba_6Ti_{17}O_{40}$. When the amount of NiO–Nb_2O_5 composite oxide was up to 0.8 mol%, a good dielectric property was achieved and satisfied the requirement of (EIA) X7R specification with dielectric constant as high as 4706 and dielectric loss lower than 1.5%. This material is promising for preparing X7R MLCCs with large capacitances.

Acknowledgments

This work was supported by Program for New Century Excellent Talents in University (NCET) and 863 program (2007AA03Z423).

References

[1] Y. Yuan, S.R. Zhang, X.H. Zhou, Effects of Nb_2O_5 doping on the microstructure and the dielectric temperature characteristics of barium titanate ceramics, J. Mater. Sci. 44 (2009) 3751–3757.

[2] H. Kishi, Y. Okino, M. Honda, et al., The effect of MgO and rare-earth oxide on formation behavior of core–shell structure in $BaTiO_3$, Jpn. J. Appl. Phys. 36 (1997) 5954–5957.

[3] W. Li, J.Q. Qi, Y.L. Wang, L.T. Li, Z. Gui, Doping behaviors of Nb_2O_5 and Co_2O_3 in temperature stable $BaTiO_3$-based ceramics, Mater. Lett. 57 (2002) 1–5.

[4] Y.H. Song, H.J. Hwang, Y.H. Han, Effects of Y_2O_3 on temperature stability of acceptor-doped $BaTiO_3$, Jpn. J. Appl. Phys. 44 (2005) 1310–1313.

[5] P.P. Phulea, S.H. Risbud, Low temperature synthesis and dielectric properties of ceramics derived from amorphous barium titanate gels and crystalline powders, Mater. Sci. Eng. B 3 (1989) 241–247.

[6] C.T. Xia, E.W. Shi, W.Z. Zhong, J.K. Guo, Hydrothermal synthesis of $BaTiO_3$ nano/microcrystals, J. Cryst. Growth 166 (1996) 961–966.

[7] X.H. Wang, R.Z. Chen, Z.L. Gui, L.T. Li, The grain size effect on dielectric properties of $BaTiO_3$ based ceramics, Mater. Sci. Eng. B 99 (2003) 199–202.

[8] M.B. Park, S.J. Hwang, N.H. Cho, Effect of the grain size and chemical features on the phase transition and physical characteristics of nano-grained $BaTiO_3$ ceramics, Mater. Sci. Eng. B 99 (2003) 155–158.

[9] H.I. Hsing, K.Y. Yin, F.S. Yen, C.Y. Hwang, Effects of particle size of $BaTiO_3$ powder on the dielectric properties of $BaTiO_3$/polyvinylidene fluoride composites, J. Mater. Sci. 36 (2001) 3809–3815.

[10] W. Zhu, C.C. Wang, S.A. Akbar, R. Asiaie, Fast-sintering of hydrothermally synthesized $BaTiO_3$ powders and their dielectric properties, J. Mater. Sci. 32 (1997) 4303–4307.

[11] A.B. McInroy, et al., Enhanced microwave-assisted sintering of X7R ceramic dielectrics for use in multilayer capacitors, Ceram. Int. 36 (2010) 2007–2010.

[12] N. Kikuchi, T. Ogasawara, S. Iwaya, Development of dielectric material with X8R characteristic, Ceram. Trans. 32 (1993) 191–200.

[13] H. Chazono, H. Kishi, Sintering characteristics in $BaTiO_3$–Nb_2O_5–Co_3O_4 ternary system, J. Am. Ceram. Soc. 82 (1999) 2689–2697.

[14] S. Wang, S.R. Zhang, X.H. Zhou, B. Li, Z. Chen, Investigation on dielectric properties of $BaTiO_3$ co-doped with Ni and Nb, Mater. Lett. 60 (2006) 909–911.

[15] W.H. Tzing, W.H. Tuan, Effect of NiO addition on the sintering and grain growth behavior of $BaTiO_3$, Ceram. Int. 25 (1999) 69–75.

[16] J.Q. Huang, P.Y. Du, W.J. Weng, G.R. Han, Effect of doped Ni^{2+} on the dielectric properties of NiO–$BaTiO_3$ composites, J. Electroceram. 21 (2008) 394–397.

[17] E. Brzozowski, M.S. Castro, Grain growth control in Nb-doped $BaTiO_3$, J. Mater. Process. Technol. 168 (2005) 464–470.

[18] M. Kahn, Influence of grain growth on dielectric properties of Nb-doped $BaTiO_3$, J. Am. Ceram. Soc. 54 (1971) 455–457.

[19] R.Z. Chen, X.H. Wang, L.T. Li, Z.L. Gui, Effects of Nb/Co ratio on the dielectric properties of $BaTiO_3$-based X7R ceramics, Mater. Sci. Eng. B 99 (2003) 298–301.

[20] W.H. Tzing, W.H. Tuan, Dielectric properties of NiO-doped $BaTiO_3$ sintered with different oxygen partial pressure, Key Eng. Mater. 132–136 (132) (1997) 1167–1170.

[21] Y.M. Chiang, D.P. Birnie, W.D. Kingery, Physical Ceramics, John Wiley & Sons, New York, 1997.

[22] C.R. Zhoua, X.Y. Liu, Effect of B-site substitution by $(Ni_{1/3}Nb_{2/3})^{4+}$ for Ti^{4+} on microstructure and piezoelectric properties in $(Bi_{1/2}Na_{1/2})TiO_3$ piezoelectric ceramics, J. Alloys Compd. 466 (2008) 563–567.

[23] Y. Park, Y.H. Kim, H.G. Kin, The effect of grain size on dielectric behavior of $BaTiO_3$ based X7R material, Mater. Lett. 28 (1996) 101–106.

[24] M.I. Mendelson, Average grain size in polycrystalline ceramics, J. Am. Chem. Soc. 52 (1969) 443–446.